Laser-based surface multistructuring using optical elements and the Talbot effect

María Aymerich,[1] Daniel Nieto,[1,*] and María Teresa Flores-Arias[1,2]

[1]*Microoptics and GRIN Optics Group, Applied Physics Department, Faculty of Physics, University of Santiago de Compostela, Santiago de Compostela, E15782, Spain*

[2]*maite.flores@usc.es*

[*]*daniel.nieto@usc.es*

Abstract: We present a laser based technique combined with the Talbot effect for microstructuring surfaces. The use of the Talbot effect is introduced as a solution to avoid damage of the periodic object used for micropattering different surfaces during the ablation process. The fabrication of two periodic objects (a mask and a microlens array) for micropattering surfaces and the identification of their Talbot planes is presented. A metal foil is ablated at distances corresponding to selected Talbot planes of the periodic objects. The setup allows us to design the desired pattern and the result is a multistructured surface with a high number of identical microholes, achieving a minimum diameter around 4μm. The different aspect of the periodic object working in direct contact and working at these Talbot distances is shown. These pictures reveal the advantages of working of using Talbot effect for a rapid, repeatable and no-contaminant multistructuring. Some industrial applications are illustrated.

OCIS codes: (140.3390) Laser materials processing; (070.6760) Talbot and self-imaging effects; (220.4000) Microstructure fabrication; (230.3990) Micro-optical devices; (350.3950) Micro-optics.

References and links

1. V. Romano, H. P. Weber, G. Dumitru, S. M. Pimenov, T. V. Kononenko, V. I. Konov, H. Haefke, Y. Gerbig, M. L. Sentis, J. Hermann, S. Bruneau, and W. Marine, "Laser surface microstructuring to improve tribological systems," in *Laser Processing of Advanced Materials and Laser Microtechnologies*, F. Dausinger, ed. (SPIE, 2003), pp.199–211.
2. D. Weibel, A. Michels, A. Feil, L. Amaral, S. Teixeira, and F. Horowitz, "Adjustable hydrophobicity of Al sustrates by chemical surface funcionalization of nano/microstructures," J. Phys. Chem. C **114**(31), 13219–13225 (2010).
3. N. C. Tien, S. Jeong, L. M. Phinney, K. Fushinobu, and J. Bokor, "Surface adhesion reduction in silicon microstructures using femtosecond laser pulses," Appl. Phys. Lett. **68**(2), 197–199 (1996).
4. M. H. Wu, C. Park, and G. M. Whitesides, "Generation of submicrometer structures by photolithography using arrays of spherical microlenses," J. Colloid Interface Sci. **265**(2), 304–309 (2003).
5. T. Akashi and Y. Yoshimura, "Deep reactive ion etching of borosilicate glass using an anodically bonded silicon wafer as an etching mask," J. Micromech. Microeng. **16**(5), 1051–1056 (2006).
6. J. Albero, L. Nieradko, C. Gorecki, H. Ottevaere, V. Gomez, H. Thienpont, J. Pietarinen, B. Päivänranta, and N. Passilly, "Fabrication of spherical microlenses by a combination of isotropic wet etching of silicon and molding techniques," Opt. Express **17**(8), 6283–6292 (2009).
7. M. Mahbubur Razzaque and M. Tanvir Rahman Faisal, "Performance of Mechanical Face Seals with Surface Micropores," J. Mech. Eng. **37**(6), 77–80 (2008).
8. S. P. Harimkar and N. B. Dahotre, "Rapid surface microstructuring of porous alumina ceramic using continuous wave Nd:YAG laser," J. Mater. Process. Technol. **209**(10), 4744–4749 (2009).
9. I. Etsion, "State of the art in laser surface texturing," J. Tribol. **127**(1), 248–253 (2005).
10. E. G. Gamaly, A. V. Rode, V. T. Tikhonchuk, and B. Luther-Davies, "Ablation of solids by femtosecond lasers: ablation mechanism and ablation thresholds for metals and dielectrics," Phys. Rev. A **9**(3), 949–957 (2001).
11. P. T. Mannion, J. Magee, E. Coyne, G. M. O'Connor, and T. J. Glynn, "The effect of damage accumulation behaviour on ablation thresholds and damage morphology in ultrafast laser micro-machining of common metals in air," Appl. Surf. Sci. **233**(1-4), 275–287 (2004).
12. A. Piqué, S. A. Mathews, B. Pratap, R. C. Y. Auyeung, B. J. Karns, and S. Lakeou, "Embedding electroniccircuits by laserdirect-write," Microelectron. Eng. **83**(11-12), 2527–2533 (2006).

#247187 Received 3 Aug 2015; revised 27 Aug 2015; accepted 1 Sep 2015; published 8 Sep 2015

13. J.-Y. Cheng, C.-W. Wei, K.-H. Hsu, and T.-H. Young, "Direct-write laser micromachining and universal surface modification of PMMA for device development," Sens. Actuators B Chem. **99**(1), 186–196 (2004).
14. N. Bityurin and A. Kuznetsov, "Use of harmonics for femtosecond micromachining in pure dielectrics," J. Appl. Phys. **93**(3), 1567–1576 (2003).
15. J. Ihlemann, "Micro patterning of fused silica by laser ablation mediated by solid coating absorption," Appl. Phys., A Mater. Sci. Process. **93**(1), 65–68 (2008).
16. A. Issa, D. Brabazon, and M. S. J. Hashmi, "3D transient thermal modelling of laser microchannel fabrication in lime-soda glass," J. Mater. Process. Technol. **207**(1-3), 307–314 (2008).
17. D. Nieto, G. Vara, J. A. Díez, G. M. O'Connor, J. Arines, C. Gómez-Reino, and M. T. Flores-Arias, ""Laser-based microstructuring of surfaces using low cost microlens arrays," J. Micro/Nanolith, MEMES MOEMS **11**(2), 023014 (2012).
18. M. He, X. C. Yuan, N. Ngo, J. Bu, and S. Tao, "Low-cost and efficient coupling technique using reflowed sol-gel microlens," Opt. Express **11**(14), 1621–1627 (2003).
19. Y. Lin, M. H. Hong, G. X. Chen, C. S. Lim, Z. B. Wang, L. S. Tan, L. P. Shi, and T. C. Chong, "Patterning of phase change films with microlens arrays," J. Alloys Compd. **449**(1-2), 253–257 (2008).
20. Y. Lin, M. H. Hong, G. X. Chen, C. S. Lim, L. S. Tan, Z. B. Wang, L. P. Shi, and T. C. Chong, "Hybrid laser micro/nanofabrication of phase change materials with combination of chemical processing," J. Mater. Process. Technol. **192-193**, 340–345 (2007).
21. C. S. Lim, M. H. Hong, Y. Lin, G. X. Chen, A. Senthil Kumar, M. Rahman, L. S. Tan, J. Y. H. Fuh, and G. C. Lim, "Sub-micron surface patterning by laser irradiation through microlens arrays," J. Mater. Process. Technol. **192**, 328–333 (2007).
22. M. V. Berry and S. Klein, "Integer, fractional and fractal Talbot effects," J. Mod. Opt. **43**(10), 2139–2164 (1996).
23. A. W. Lohmann, D. Mendlovic, and G. Shabtay, "Talbot (1836), Montgomery (1967), Lau (1948) and Wolf (1955) on periodicity in optics," Pure Appl. Opt. **7**(5), 1121–1124 (1998).
24. W. D. Montgomery, "Self-Imaging Objects on Infinite Aperture," J. Opt. Soc. Am. **57**(6), 772–778 (1967).
25. T. Delgado, D. Nieto, and M. T. Flores-Arias, "Fabrication of microlens arrays on soda-lime glass using a laser direct-write technique and a thermal treatment assisted by a CO_2 laser," Opt. Lasers Eng. **73**, 1–6 (2015).
26. K. Patorski, "The Self-Imaging Phenomenon and its applications," Prog. Opt. **27**, 1–108 (1989).
27. C. Gómez-Reino, M. V. Pérez, and C. Bao, *Gradient-Index Optics: Fundamentals and Applications* (Springer, 2002).
28. B. Besold and N. Lindlein, "Fractional Talbot effect for periodic microlens arrays," Opt. Eng. **36**(4), 1099–1105 (1997).
29. B. E. A. Teich and M. C. Teich, *Fundamentals of Photonics* (John Wiley & Sons Inc. 1991).
30. B. Besold and N. Lindlein, "Practical limitations of the Talbot imaging with microlens arrays," Pure Appl. Opt. **6**(6), 691–698 (1997).
31. A. W. Lohmann, *Optical Information Processing* (Universität Erlangen-Nijberg, 1978), pp. 107–108.
32. S. W. Zhang, "State-of-the-art of polymer tribology," Tribol. Int. **31**(1-3), 49–60 (1998).
33. V. Ijeri, K. Shah, and S. Bane, "Chromium-free etching and palladium-free plating of plastics," NASF Surf. Tech. White Pepers **78**(12), 1–8 (2014).

1. Introduction

Surface microstructuring presents a high interest in industry due to its various applications [1]. By modifying the surface of a material, tribological properties such as wettability or friction, can be altered. Therefore, a substrate can be functionalized in order to behave as hydrophobic or hydrophilic [2] or to modify its adherence can be increased or decreased [3]. Also, the surface texturing plays an important role in the process of metallization of plastics, which traditionally includes very toxic and contaminant steps.

Over the years, different forms to modify the surfaces at the micrometer and submicrometer scale were developed. Some examples of these surface texturing techniques are photolithography [4], chemical etching [5,6], face sealing [7] or laser ablation [8,9]. Laser ablation presents a great advantage among all of them: versatility, speed and the ability to adapt to a wide different range of structures without altering the properties of the material [10,11]. However, a rapid and precise control of geometrical features is necessary to obtain the full potential of the surface micropattering with laser. Due to this fact, the efforts must be focused on the implementation of rapid manufacturing techniques and, in this context, microoptics plays an important role in various industrial manufacturing process like microelectronics [12], laser-machining [13,14] and materials processing [15,16].

Some of the authors have reported the use of periodic object and microlens arrays for performing laser microstructuring [17]. In the case of the periodic object for performing the ablation of a sample with laser, a periodic object is usually employed as a mask that transfers its pattern to the substrate and it must be placed in direct contact with the sample. In the case

#247187 Received 3 Aug 2015; revised 27 Aug 2015; accepted 1 Sep 2015; published 8 Sep 2015

of the microlens array, the target is placed at the focal length of the array. In this case, each microlens of the array concentrates more energy at focus and the process is more efficient. The use of microlenses is particularly well suited for manufacturing, optimization of laser beam delivery as well as improvement of production efficiency with the intention of cost reduction [18]. In previous work some of the authors have demonstrated the structuring capabilities of microlenses arrays over a variety of different material, such as stainless steel, aluminium, copper and polymer [17]. Nevertheless, both the mask and the microlenses, present a problem of durability due to the interaction of the material expelled from the substrate during the ablative process and these elements. To avoid the rapid contamination and deterioration of the periodic object and the microlenses, it was realized that the best option will be to separate the target a distance enough for the expelled material does not reach the optical element used for the structuring. To overcome this, in this work we propose the use of the Talbot effect.

Some other authors have demonstrated in the past the possibility of combine the Talbot effect, or self-image phenomenon, with laser irradiation using optical elements in order to multistructure different materials. For example, this effect was used with an array of microlenses to structure a thin film, creating micropatterns of dots over the substrate at certain distances from it [19,20]. Also using a microlens array, materials like photoresist were microstructured with laser using the self-image phenomenon and different patterns from the one created at the focal length were obtained [21].

The Talbot effect consists of the repetition of the complex amplitude distribution of a periodic object or the foci of microlenses at several finite distances from it, called the Talbot distances, when the object is illuminated by coherent light. These Talbot distances depend on the period of the object, the wavelength and the kind of illumination employed [22]. The longitudinal repetition of the image along the optical axis does not need any optical elements, such as lens or mirrors, and it was demonstrated that not only periodic objects cause this effect, but every object that satisfies the called Montgomery conditions [23]. So, the periodicity of the object is just a sufficient but not a necessary condition. Nevertheless, the periodic objects are the most employed to observe the Talbot phenomenon [24]. In this work, we present the fabrication of a periodic object by a laser direct-write technique that after a thermal treatment turns into a microlens array. The initial periodic object and the final microlenses are employed for micro-patterning surfaces, using the Talbot effect as a tool to overcome the problem of the damage caused to the object during the ablation process since it allow us to increase the distance between periodic object and substrate. In section 2 we present the materials and methods. Section 3 is devoted to the use of the Talbot effect as a solution to the deterioration problem. In section 4 we describe some industrial applications. Section 5 presents the conclusions.

2. Materials and methods

In order to perform the microstructuring of the glass to fabricate the initial periodic object that would act as a mask, a Rofin model Nd:YVO_4 laser was used. This is a solid-state laser, operating at 1064 nm wavelength and using a Q-Switch regime, with pulses of 20 nanoseconds. Subsequently, an Easy Mark CO_2 laser system with a fundamental wavelength of 10.6μm providing a maximum power of 124W was employed to apply a post thermal treatment for obtaining the microlens array from the previous structure [25].

A confocal microscope SENSOFAR PLμ 2300 allow us to perform topographic measurements on the surface and to obtain 3D images of the generated microposts and microlenses. The results presented were acquired using a 20xEPI microscope objective, with a numerical aperture of 0.45 and a working distance of 4.5mm. The glass used as substrate for fabricating the microlens arrays was a commercial soda-lime glass, provided by a local supplier.

A He-Ne laser model JDS Uniphase 1144P is used for the identification of the Talbot planes and for choosing the most suitable, with a 20X microscope objective and a CCD camera. A Nd:YAG laser with parameters $\lambda = 532$nm, pulse width 20 ns at 50Hz and $M^2<1.2$

#247187 Received 3 Aug 2015; revised 27 Aug 2015; accepted 1 Sep 2015; published 8 Sep 2015

is employed for the surface microstructuring. The target used is a stainless steel of 1 mm thickness. A Nikon MM-400 microscope is used for the visual characterization and a scanning electron microscope FESEM ZEISS ULTRA PLUS is used to achieve images of the periodic objects after ablation.

3. Talbot effect

The aim of this work is to multistructure different surfaces using a simple and efficient technique. Is well known that the Talbot effect is a diffraction phenomena that occurs for periodic object and consists of the repetition of the image at certain distances from the object with no need of any optical elements [26]. Our purpose is to use by one hand a mask fabricated by laser direct-writing and by the other hand the foci of a microlens array obtained after expose the initial structure fabricated to a thermal treatment as periodic object for the Talbot object. If we place the surface to be structured at the axial length corresponding to the integer Talbot distances, we obtain the same multistructure pattern than if it is placed in direct contact for the first case proposed or if the substrate is at the focal plane of the microlenses in the second case. Using this approach we increase the distance between the object and the target, avoiding that the material expelled from the target damage the elements.

Firstly, we identify Talbot images of the periodic objects (the mask and the foci) when are illuminated by the He-Ne laser. The Talbot distances depend on the period of the object, the wavelength and the kind of illumination employed. A plane wave is chosen as incident wave because is the most simple kind of illumination for which the Talbot condition can be calculated, and the Talbot distances are given by [27]

$$z_T = n\frac{p^2}{\lambda}. \tag{1}$$

where z_T is the distance between the periodic object and the Talbot image, n is an integer, p is the period of the object and λ is the wavelength of illumination

When an array of microlenses is used as periodic object, the Talbot distances measured from the object are given by [28]

$$z = f_{ML} + z_T. \tag{2}$$

where f_{ML} is the foci of the microlens and z_T is the Talbot distance. The magnification for this kind of illumination is the unity. We use a He-Ne laser for the identification of the Talbot planes, because can easily be recorded than when use a pulsed power laser for multistructuring different targets.

3.1 Fabrication of periodic objects

We manufacture the periodic objects that are employed in this work because in this way we can perform design the structure we want increasing the versatility of the processed technique. Firstly, a periodic object that acts as a mask is fabricated in a commercial soda-lime glass by a laser direct-write technique with a Q-Switch Nd:YVO_4 laser with a fundamental wavelength of 1063nm. Through the movement of the laser beam, controlled by a galvanometer mirror system, cylindrical microposts are fabricated by direct laser ablation of circular trenches (Fig. 1(a)). Laser parameters were: average power 7W, repetition rate of 9kHz and scan speed of 70mm/s. The packing pattern of the array of microposts is a hexagonal pattern with 50μm period. This periodic object is going to be employed in the next section as a mask that transfers its pattern to the substrate to be structured.

If this initial periodic object is exposed to a thermal treatment (Fig. 1(b)) we can obtain an array of microlenses and use its foci as the periodic object that repeats its image along the propagation axis. By using a roller furnace combined with a CO_2 laser, the material at the top of the microposts achieves the transition temperature of the soda-lime glass and reduces its viscosity. Consequently, the surface tension of the melted material induces the modification of the surface shape while the rest of the substrate remains at a lower temperature. The

#247187 Received 3 Aug 2015; revised 27 Aug 2015; accepted 1 Sep 2015; published 8 Sep 2015

original microposts become spherical microlenses with good optical quality [25]. Lasers parameters were: wavelength of 10.6μm, repetition rate of 10kHz and a scan speed of 350cm/s.

Figure 1 shows setups used for the fabrication of the periodic objects. The profile of the mask obtained by a laser direct ablation can be observed in Fig. 1(c). The thermal treatment to achieve the microlenses is described in Fig. 1(b) and the final profile is shown in Fig. 1(d). By this manufacturing process we can fabricate the two different periodic objects that are employed in this work. The topographic measurements were done with a confocal microscope SENSOFAR PLμ 2300.

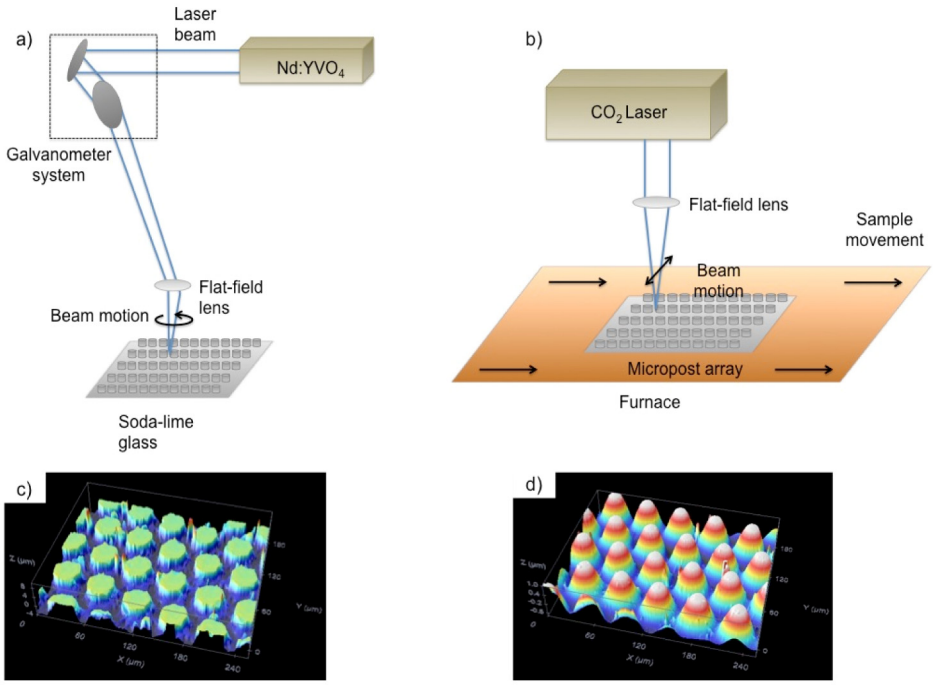

Fig. 1. a) Experimental setup for the fabrication of the mask by a laser direct-write technique, b) experimental setup of the thermal treatment for achieving the microlenses array, c) confocal image of the microposts structure after the laser ablation and d) confocal image of the microlenses after the thermal treatment.

3.2 Identification of the self-images

Now that the periodic objects are fabricated, we proceed to the identification of Talbot planes. We look for those images that shown a uniform irradiance profile. The position of the self-images must attend to Eq. (1) under plane wave illumination and the theoretical formula has to be verified experimentally. For this purpose, the setup described in Fig. 2 was used.

#247187 Received 3 Aug 2015; revised 27 Aug 2015; accepted 1 Sep 2015; published 8 Sep 2015

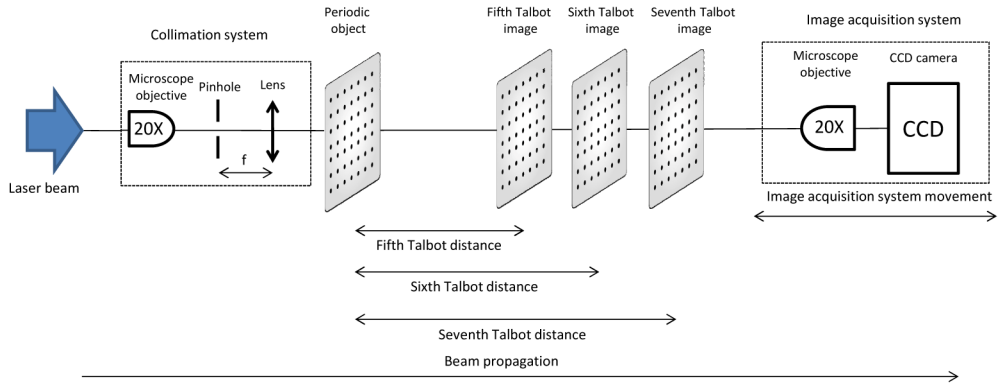

Fig. 2. Experimental setup for the identification of the Talbot images when a periodic object is illuminated by a HeNe laser. The laser beam passes through a collimation system (formed by a 20X microscope objective; a spatial filter and a lens), that illuminates the periodic object. The image system acquisition for capturing the Talbot images is formed by a 20X microscope objective and a CCD camera. The image acquisition system is moved laterally to capture the different Talbot images.

Figure 2 shows the experimental setup for the verification of the Talbot distances when a mask is used as periodic object. The laser beam is collimated by using a 20X microscope objective that concentrates the light on a pinhole that acts as spatial filter. The pinhole is placed at the focal length of a convergent lens. The collimated beam illuminates the periodic object. This object is fabricated over a soda-lime glass substrate. The Talbot images are acquired with an image system formed by a 20X microscope objective and a CCD camera. The acquisition image system is moved laterally at the theoretical Talbot distances, corresponding to the fifth ($z_5 = 19.75 \pm 0.03$mm), sixth ($z_6 = 23.75 \pm 0.03$mm) and seventh ($z_7 = 27.70 \pm 0.03$mm) Talbot images. The irradiance distribution of each plane is recorded by the CCD camera.

When the focal plane of the microlens array is used as periodic object, the setup used for the identification of the Talbot images of the foci is described at Fig. 3.

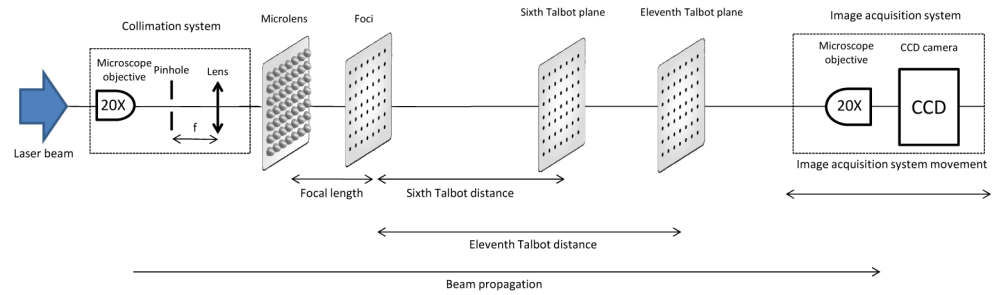

Fig. 3. Experimental setup for the identification of the Talbot images when a microlens array is illuminated by a HeNe laser. The collimation system is the same that this described in Fig. 2 as well as the image system acquisition. Note that the periodic object used for the Talbot effect is the focal plane of the microlens array.

When the focal plane of the array of microlenses is used as periodic object, the value of the focal length 0.34 ± 0.03mm in our case, needs to be add up to the theoretical value of the Talbot distance for taking the origin of measurement at the microlens array. The setup consists of the same elements as in the case of the mask (Fig. 2) and the acquisition image system is placed at distances calculated theoretically by Eq. (2), that is at 24.07 ± 0.03mm for the sixth Talbot plane and 43.79 ± 0.03mm for the eleventh one.

#247187 Received 3 Aug 2015; revised 27 Aug 2015; accepted 1 Sep 2015; published 8 Sep 2015

Figure 4 shows the Talbot images when the mask is used and Fig. 5 presents the images obtained in the case we use the microlens array. The images were obtained with an acquisition image system provided with a 20X microscope objective.

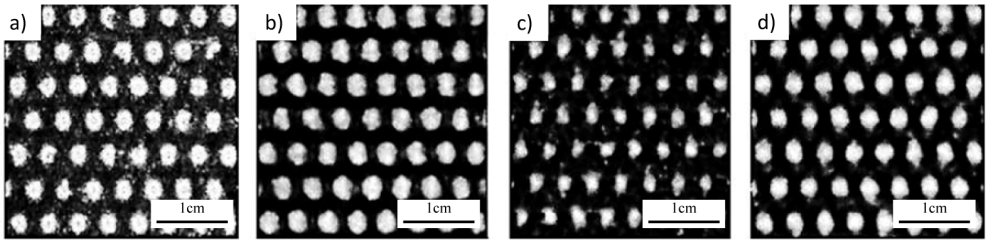

Fig. 4. CCD-images of the mask obtained with the experimental setup that employs a HeNe laser a) object, b) fifth Talbot plane, c) sixth Talbot plane and d) seventh Talbot plane.

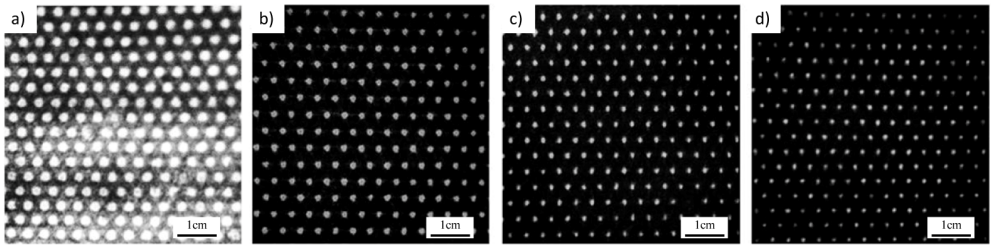

Fig. 5. CCD-images of the microlens array obtained with the experimental setup that employs a HeNe laser a) object, b) foci of the microlenses, c) sixth Talbot plane and d) eleventh Talbot plane.

Figures 4 and 5 permit us to say that the theoretical values are in good agreement with the experimental results. Moreover, in both cases the magnification of the image is the unity as expected. Figure 4(c) shows a worse image in term of the homogeneity of the irradiance distribution than in the other cases. This could be because of a mild discrepancy between the theoretical value and the experimental position. Nevertheless, the image of the mask is repeated and the hexagonal pattern is obtained.

4. Surface multistructuring

After the selection of the Talbot planes that present a more homogenium aspect we proceed to microstructure different materials. In order to have energy enough to structure the substrates, we use a more power Nd:YAG Q-switch laser (see section II), commonly employed in industrial applications.

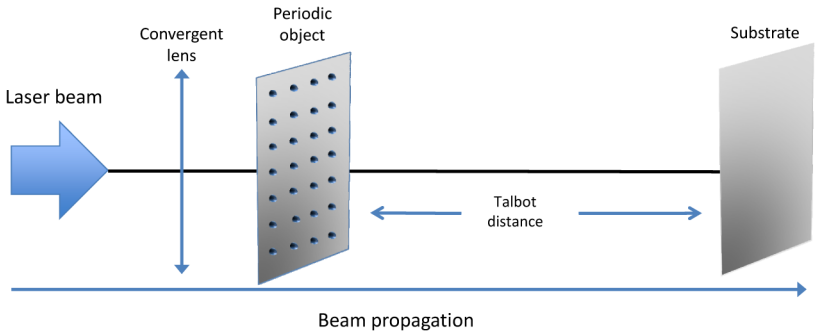

Fig. 6. Experimental setup for performing the surface ablation with a Nd:YAG laser and the mask. The laser beam passes through a convergent lens and illuminates the mask. The substrate is placed at the theoretical Talbot distances from the object.

#247187 Received 3 Aug 2015; revised 27 Aug 2015; accepted 1 Sep 2015; published 8 Sep 2015

Figure 6 depicts the setup employed for the microstructuring of the surface when the mask is used as periodic object. It is formed by a Nd:YAG working at its second harmonic (λ = 532nm), with a pulse width of 20ns at 50Hz and M^2<1.2 and a convergent lens of 7cm focal length located at 3.5 ± 0.1cm from the object, that allow us to increase the irradiance on the target. The mask and the substrate will be separated by a distance equal to the chosen Talbot distance.

When the focal plane of the microlens is employed as the periodic periodic object, we must take into account the approximation given by Eq. (2), so the resulting setup for the surface ablation is shown in Fig. 7. In this case the lens is placed at 4.5 ± 0.1cm from the object.

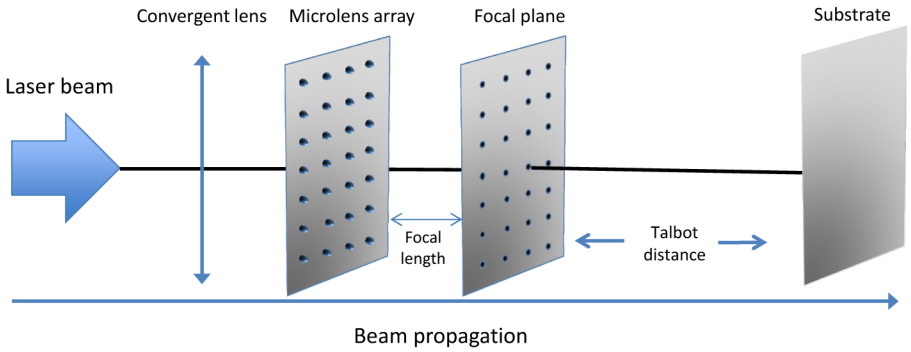

Fig. 7. Experimental setup for performing the surface ablation with a Nd:YAG laser and the microlens array. The laser beam passes through a convergent lens and illuminates the microlenses. The substrate is placed at the theoretical Talbot distances measured from the foci.

In both setups, we have to take into account that the kind of illumination has changed respect to the He-Ne case, it is no longer a plane wave, so the condition for the Talbot distances must be calculated again. We assume that a plane Gaussian beam emerges from the laser and passes through the lens, obtaining a new Gaussian beam with different parameters. The radii of curvature of the beam after the lens has been approximated by the distance between the lens and the object [29]. After solving the diffraction integral for this case, the Talbot condition is given by

$$n\frac{p^2}{\lambda}=\frac{R-z_T}{R}z_T. \tag{3}$$

where R is the radii of curvature of the Gaussian beam. So the Talbot distances for this kind of illumination is

$$z_T=\frac{R+\sqrt{R^2-4Rp^2n/\lambda}}{2}. \tag{4}$$

where the positive sign has been chosen for recovering the initial conditions, because the radii takes a negative value because it is convergent. Again, if we want to find the self-images of the foci of the microlenses, the repetition of the foci will be found at positions z from the array such as

$$z=f_{ML}+z_T. \tag{5}$$

As the illumination has changed and a lens is placed to have enough energy for perform the ablation, the magnification is no longer the unity. In fact, in our case we will obtain self-images with magnification below the unity. The formula for the magnification is given by the ratio between the position of the self-image and the position of the object [27]

#247187 Received 3 Aug 2015; revised 27 Aug 2015; accepted 1 Sep 2015; published 8 Sep 2015

$$M = \frac{R + z_T}{R}. \tag{6}$$

where R is the distance from the periodic object and the lens and z_T is the Talbot distance. In our case the value of R has a negative sign to indicate that the light converges.

Once we achieved the theoretical formula for the distances with the Nd:YAG setup, these theoretical values must be verified experimentally. We use the setup shown in Fig. 6 when we use a mask as a periodic object and the one described in Fig. 7 when a microlens array is employed. We also include a 40X microscope objective between the periodic object and the image in order to magnify and record the image. In each case, we place the observation plane at the distances predicted theoretically. For the mask, these distances correspond to 16.09 ± 0.03mm for the fifth Talbot plane, 18.45 ± 0.03mm for the sixth and 20.67 ± 0.03mm for the seventh. For the microlenses, the theoretical values correspond to 20.26 ± 0.03mm for the sixth Talbot plane and 31.63 ± 0.03mm for the eleventh. The CCD-images for the mask and the microlens array are shown in Figs. 8 and 9, respectively. The images were obtained with an acquisition image system provided with a 40X microscope objective.

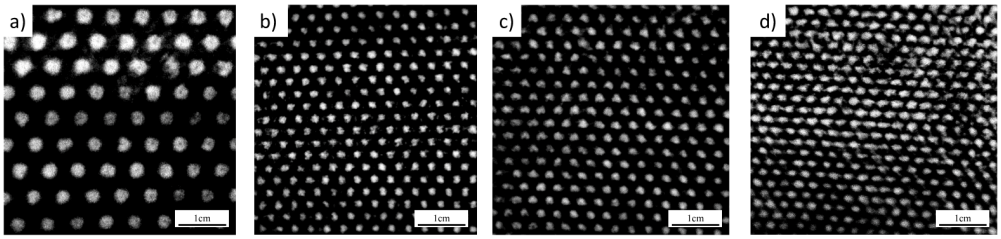

Fig. 8. CCD-images of the mask obtained with the experimental setup that employs a Nd:YAG laser a) object, b) fifth Talbot plane, c) sixth Talbot plane and d) seventh Talbot plane.

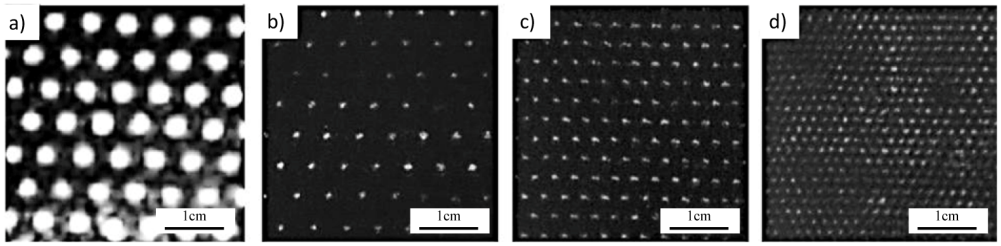

Fig. 9. CCD-images of the microlens array obtained with the experimental setup that employs a Nd:YAG laser a) object, b) foci of the microlenses, c) sixth Talbot plane and d) eleventh Talbot plane.

The tolerances (RMS values) of the Talbot planes in engraving mask were evaluated to be a 0.18%, 0.16% and 0,14% for the fifth, sixth and seventh Talbot image, respectively. In the case of the microlenses, the tolerances were achieved to be 0.15% and 0.09% for the sixth and eleventh Talbot planes, respectively. As it was expected the tolerance decrease as the axial distance increases. Moreover, the high order Talbot images would not have energy enough for performing patterning by laser ablation on the substrate materials presented in this paper. The walk-off effect was not considered in this paper because the number of illuminated elements of the periodic object is high enough to produce the Talbot images used in this work [28,30,31].

From Figs. 8 and 9, we realise that the magnification is no longer the unity and that the period of the image decreases as long as we increase the Talbot order. For the mask, these theoretical values of the magnification correspond to $M_5 = 0.54$ for the fifth Talbot image, $M_6 = 0.47$ for the sixth and $M_7 = 0.41$ for the seventh. For the microlenses, the theoretical values correspond to $M_6 = 0.58$ for the sixth Talbot image and $M_{11} = 0.35$ for the eleventh. This

#247187 Received 3 Aug 2015; revised 27 Aug 2015; accepted 1 Sep 2015; published 8 Sep 2015

decrease of the magnification causes a blur of the image and consequently, a deterioration of it.

Once the Talbot distances are known and verified, we proceed to the ablation of a metal surface with a laser. The setups used are the ones described in Figs. 6 and 7. The substrate is a stainless steel of 1mm of thickness and it is placed at the theoretical Talbot distances. The laser parameters for ablation are: pulse repetition rate of 50Hz and energy per pulse of 450μJ. This energy is enough to structure the metal foil with the presented setups. Figure 10 shows the optical images of the microholes created using the mask when the stainlees steel foil is placed at distances 16.09 ± 0.03mm, 18.45 ± 0.03mm and 20.67 ± 0.03mm from the object, corresponding to the fifth, sixth and seventh Talbot distances respectively. The time of processing is around 7 seconds.

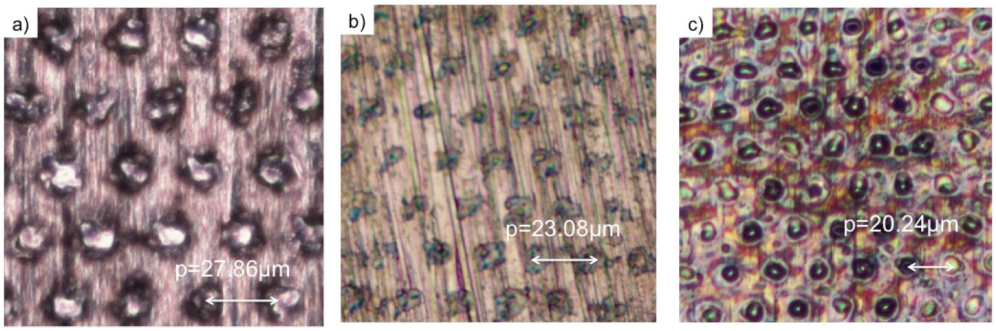

Fig. 10. Images obtained after the ablation of a foil of stainless steel with thickness of 1mm using the mask when the surface is placed at a distance corresponding to a) the fifth Talbot plane, b) sixth Talbot plane and c) seventh Talbot plane from the object. The period p is indicated in the images. The images were obtained with a microscope in reflected mode and bright field.

As you can see in Fig. 10, by illuminating the periodic object presented in Fig. 1(c) with a Nd:YAG laser beam, we use the fifth, sixth and seventh Talbot images to structure a metal foil of thickness 1 mm. It is visible in this figure that the magnification is not the unity, as it was expected. The magnification attends to Eq. (6) and the original period of 50μm of the object now decreases, with theoretical values of 27.01μm for the fifth Talbot distance, 23.62μm for the sixth and 20.45μm for the seventh, which are in good agreement with the experimental ones that are shown in Fig. 10. Also, the diameter of the microspot decreases with values of 8.62 ± 0.10μm when it is placed in the fifth, 6.48 ± 0.10μm in the sixth and 5.71 ± 0.10μm in the seventh. The deep of the microholes is around 1μm.

Figure 11 shows the micropattering obtained when the microlens array is employed and the substrate, a stainless steel of 1mm thickness, is placed at distances 0.34 ± 0.03mm (focal length), 20.26 ± 0.03mm (sixth Talbot distance) and 31.63 ± 0.03mm (eleventh Talbot plane) from the object. The exposition time it is around 7 seconds.

#247187 Received 3 Aug 2015; revised 27 Aug 2015; accepted 1 Sep 2015; published 8 Sep 2015

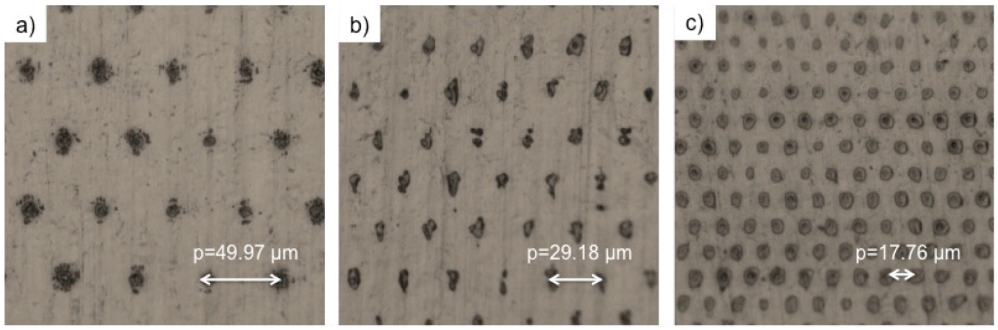

Fig. 11. Images of the microholes obtained after the ablation of a foil of stainless steel with thickness of 1mm using the foci of the microlenses when the surface is placed at a distance equal to a) the foci of the microlens, b) sixth Talbot plane and c) eleventh Talbot from the object. The period p is indicated in the images. The images were obtained with a microscope in reflected mode and bright field.

Figure 11 shows the obtained patterns when the stainless steel foil of 1mm thickness is placed at a distance equal to the focal length (Fig. 11(a)) and at the sixth and eleventh Talbot distances, respectively (Figs. 11(b) and 11(c)). As predicted, the period is different since the magnification changes. In particular, the period of the pattern decreases as long as the Talbot order increases due to the fact that the magnification is below the unity for this kind of illumination. The theoretical period of the ablation patterns can be calculated from the magnification given by Eq. (6), so we obtain that the period for the sixth self-image of the foci would be 29.24µm and 17.40µm for the eleventh. These results are in good agreement with those shown in Fig. 9. The diameter of the hole also decreases as the Talbot plane increases, taking a value of 6.69 ± 0.10µm for the sixth plane and 4.68 ± 0.10µm for the eleventh. The microholes have around 1µm depth.

In order to ensure the integrity of the optical elements, the samples were analysed using an electronic SEM microscope. Figures 12 and 13 show the optical elements working at a Talbot distance and working in direct contact in the case of the mask and at a focal length in the case of the microlenses, respectively. Since the mask is fabricated by laser ablation, the interstices among each micropost are not highly transparent and a small opacity remains. This fact allows us to work in direct contact. In the case of the microlens, it would be not possible because after applying the thermal treatment, the interstitial areas become transparent.

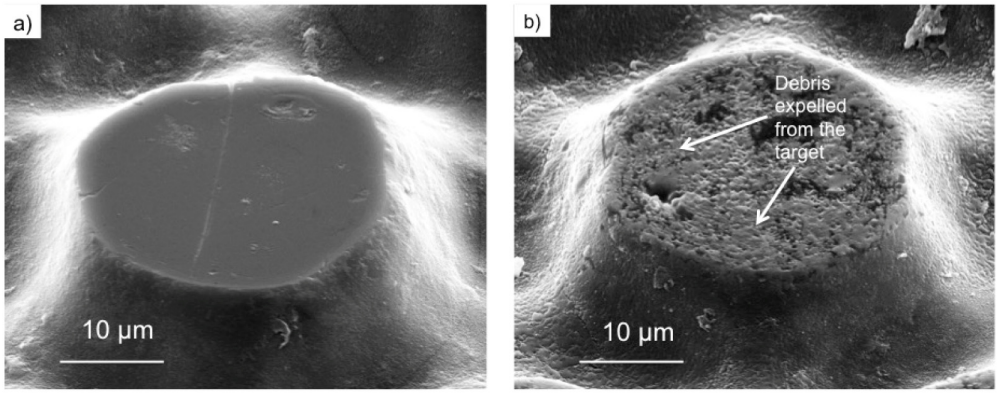

Fig. 12. SEM images of one micropost when the microstructuring was performed at a) the Talbot planes presented in Fig. 10 and b) direct contact.

#247187 Received 3 Aug 2015; revised 27 Aug 2015; accepted 1 Sep 2015; published 8 Sep 2015

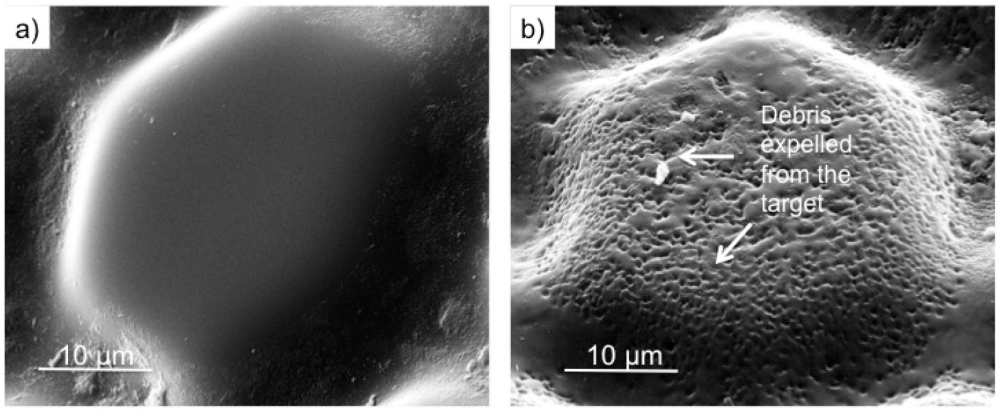

Fig. 13. SEM images of one microlens when the microstructuring was performed at a) Talbot planes shown in Fig. 11 and b) the focal plane.

We can see in Fig. 12 that when ablation is performed in a Talbot plane from the mask the periodic objects remains practically intact (Fig. 12(a)) meanwhile when we work in direct contact, the mask results damaged (Fig. 12(b)) It is clear in Fig. 13 that if the substrate is placed in the foci of the microlens array, the array suffers several damages due to the expelled particles for the substrate foil (Fig. 13(b)). As consequence, the periodic object results damaged and its useful life decreases. If the ablation is performed in a Talbot plane, the particles expelled do not damage the array and the quality of the object is kept (Fig. 13(a)). Although this process can be improved by using low absorption and high quality optical material, the low cost of the material and fabrication process makes this technique attractive compared with other methods.

4.1 Industrial applications

Surface microstructuring by laser ablation allows to generate a high number of identical structures in a short exposition time and in a no contaminant ambient. This technique is employed in several industrial applications but with the inconvenient of the rapid deterioration of the objects that transfers the geometry to the system. The Talbot effect has been presented as a possible solution that allows to separate the periodic object from the substrate. As a consequence, the damage in the objects can be avoided and they can be employed at series laser surface texturing processes.

The possibility of microstructuring surfaces with laser over different materials avoiding the damage of the periodic object that transfers the patterns presents numerous applications in industry, where a rapid, precise and cheap technique is require to modify the tribological properties of different substrates to adapt them to the diverse needs from different fields. Avoiding the replacement of the damaged periodic object very often, cost can be reduced. Figure 14 depicts the same ablation pattern that corresponds to the sixth Talbot distance of the mask over different substrates in order to illustrate the different applications of the modification of the surface.

#247187 Received 3 Aug 2015; revised 27 Aug 2015; accepted 1 Sep 2015; published 8 Sep 2015

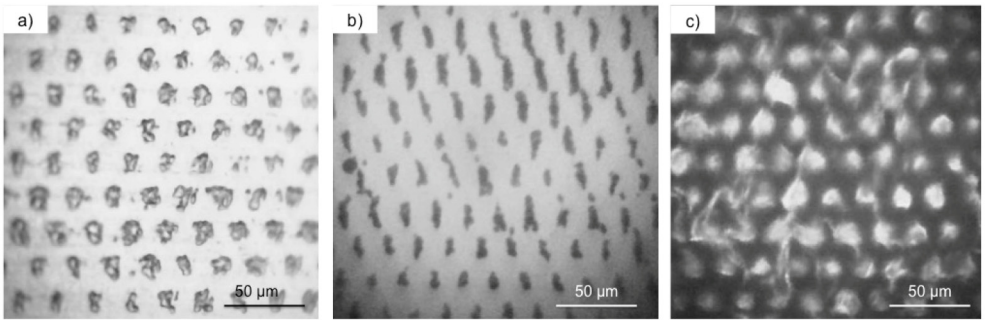

Fig. 14. Images with a metallurgic microscope of the ablation over a) a 1mm thick stainless steel foil, b) a soda-lime glass substrate with a coat of cooper of 1µm of thickness and c) a polypropylene substrate of 0.5mm. Each substrate is placed at the sixth Talbot distance from the mask. The images were obtained with a microscope in reflected mode and bright field.

Figure 14(a) shows a micropattern performed on a metal substrate, a stainless steel foil. The microstructuring of these surfaces at a micrometric level is necessary to modify the tribological properties of the material. The generation of microholes in these substrates is useful to create microstructures that act as traps for abrasive particles when two surfaces are in contact. They also act as a reservoir of lubricant liquid in friction [9]. The size and distribution of these holes is a determinant factor to calculate the friction forces between two structures, which can be easily controlled by the design of the periodic object that creates the holes.

In Fig. 14(b) we can see how the cooper coat has been eliminated selectively. The pattern is not as clear as in other materials but the result obtained can be used to generate new objects that act as masks in diverse processes such as photolithography.

Plastic surfaces, as the polypropylene one we can see in Fig. 14(c), are widely employed in processes like sealing, gears fabrication, artificial joints, engines or automation machinery that require a precise alteration of the tribological properties of the material [32]. Nowadays, plastic replace a lot of metal pieces because of weight, cost or design reasons, so industry metallizes the polymer for aesthetic motives or to make the piece conductor. We can find metallized plastic in the motoring area, in accessories for construction, decorative elements, etc. In order to metallize the plastic, the surface of the material must be altered because the adhesion of the metal to this surface is purely mechanic and not atomic. One of the most common techniques for the preparation of the substrate is the chemical etching that includes hexavalent chromium and palladium in the process, which are very toxic components [33]. For this reason, it is very interesting to look for new ways to make this process without any contaminants. Surface texturing for its metallization using chemical agents can be replace by a laser microstructuring technique as the one proposed in this work, which is no-contaminant at all, combined with the Talbot effect to avoid the damage of the periodic object.

5. Conclusions

In this paper, we have created a mask formed by microposts by a direct-write laser technique with a Nd:YVO_4 laser and a microlens array by exposing the mask to a thermal treatment with a CO_2 laser. The mask and the focal plane of the microlens array were employed to fabricate a high number of identical structures onto a substrate by laser ablation in a short exposition time. The use of the Talbot effect in this procedure allows to increase the distance from the object to the target resulting in a decreasing of the deterioration caused by the particles spelled from the substrate during the ablation process of the target and therefore, the useful life of the periodic object is increased.

#247187 Received 3 Aug 2015; revised 27 Aug 2015; accepted 1 Sep 2015; published 8 Sep 2015

Acknowlegments

This work has been supported by the Consellería de Cultura, Xunta de Galicia/FEDER, Spain under Contract EM2012/019.

#247187 Received 3 Aug 2015; revised 27 Aug 2015; accepted 1 Sep 2015; published 8 Sep 2015